J Polym Res (2011) 18:2109–2117
DOI 10.1007/s10965-011-9621-7

ORIGINAL PAPER

Shape-memory behavior of poly (methyl methacrylate-co –N-vinyl-2-pyrrolidone) / poly (ethylene glycol) semi-interpenetrating polymer networks based on hydrogen bonding

Guoqin Liu · Weichun He · Yuxing Peng · Hesheng Xia

Received: 1 November 2010 / Accepted: 26 April 2011 / Published online: 7 May 2011

Abstract Based on hydrogen bonding interactions, Poly (methyl methacrylate-co-N-vinyl-2-pynolidone) (P(MMA-co-VP)) networks and linear poly(ethylene glycol) (PEG) can form semi-interpenetrating polymer networks (semi-IPNs), i.e. P(MMA-co-VP)/PEG semi-IPNs, which has shape memory behaviour; its maximum storage modulus ratio can be more than 400, and its shape recovery ratio could reach 99%. The morphology, thermal behaviors and dynamic mechanical properties of P(MMA-co-VP)/PEG semi-IPNs were studied by FTIR, TEM, DSC and DMA. When PEG with higher molecular weight was introduced into P(MMA-co-VP) networks, they possess higher glassy state modulus and higher recovering rate. In such a system, the maximum molecular weight of PEG required for the semi-IPN formation reaches 1000.

Keywords Shape-memory · Poly (methyl methacrylate-co –N-vinyl-2-pyrrolidone) · Poly(ethylene glycol) · Semi-interpenetrating polymer networks · Hydrogen bonding

G. Liu (✉) · W. He
College of Material Science and Engineering,
Henan University of Technology,
Zhengzhou 450007, China
e-mail: guoqin_liu@haut.edu.cn

Y. Peng
Chengdu Institute of Organic Chemistry,
Chengdu 610041, China

H. Xia
State Key Lab of Polymer Materials Engineering,
Sichuan University,
Chengdu 610065, China

Introduction

Shape memory properties provide a very attractive insight into material science, opening unexplored horizons and giving access to unconventional functions in materials class. Shape memory materials are able to recover their original shape at the presence of the right stimulus [1]. Although shape memory alloys have received wide attention all the time, the rise of shape-memory polymers by far surpasses metallic shape-memory alloys in some aspects [2–9]. It is well-known that the glass transition temperature (T_g) characterizes polymers, making them unique in contrast to metals or ceramics [10]. The advantages of polymers are their easier availability and their wide range of mechanical and physical properties. Shape-memory polymers can respond to changes in the external conditions such as temperature, moisture, solvent, pH, ionic strength, and so on [11–16], which makes them desirable for a multitude of applications, including drug-delivery system, biocatalysts, biosensors, etc [17–19]. A very promising future applications of shape-memory polymers is the area of biomaterials [13, 20, 21]. A change in shape caused by a change in temperature is called a thermally induced shape-memory effect. Its mechanism can be described: a shape-memory polymer can retain temporary shape after deformation at the temperature above its T_{trans} (i.e., switching transition temperature), followed by cooling to laboratory temperature, and stress removing; after repeating heating above T_{trans}, the polymer material returns to its original shape. The transition temperature can either be a glass transition temperature (T_{g}) of polymer or a melting temperature (T_{m}) of polymer crystal. Consequently, a lot of thermally induced shape-memory polymers have been synthesized [1, 9–14, 17].

The polymers designed to exhibit a shape-memory effect require two components on the molecular level: crosslinks to determine the permanent shape and switching segments with T_{trans} to fix the temporary shape [1]. Up to now, many papers on the thermally induced shape-memory polymers introduce switching segments with the covalent linking method [9–16] and few cases concern non-covalent interaction [11, 22–24].

Polycarboxylic acids can form intermacromolecular complexes with PEG due to the hydrogen bond between the carboxyl groups of polycarboxylic acids and the ether oxygen atoms of PEG [25]; based on this type of interactions, we have succeeded in designing the hydrogen-bonded polymer network-PEG complex for shape memory network [23, 24].

Poly(*N*-vinyl-2-pyrrolidone) (PVP) can form stable complexes with PEG through hydrogen bonds between the carbonyl groups of PVP and the terminal hydroxyl groups of oligomeric PEG [26]. Here, we report a shape memory polymer with semi-IPNs in detail, i.e., poly(methyl methacrylate-co-N-vinyl-2-pynolidone) (P(MMA-co-VP)) networks/linear PEG semi-IPNs based on hydrogen bonds interaction between PVP and PEG, different from the hydrogen bonds of our previous systems [23, 24]. As a comonomer with *N*-vinyl-2-pyrrolidone, MMA has been selected due to its hydrophobic character. In the semi-IPNs, crystalline aggregates cannot be found, although PEG is a semicrystalline polymer. We believed this kind of materials can be designed as one kind of potential biomaterials for use in medicine and in other applications interfacing with biological systems, and may broaden the list of shape memory polymers.

Because PVP and PEG contain only electron-donating groups in their repeat units, it is therefore no wonder that PVP has been shown to be immiscible with high molecular weight PEG [27]. Our experiments also show a same result. In such semi-IPNs, the maximum molecular weight of PEG required reaches to 1000.

Experimental section

Materials

Methyl methacrylate (MMA) and 2, 2′-azobis(isobutyronitrile) (AIBN) were of analytical grade obtained from the Chengdu Reagent Factory. Ethylene glycol dimethacrylate (EGDMA) and *N*-vinyl-2-pyrrolidone (NVP) were purchased from Aldrich Chemical Co. MMA was distilled under reduced pressure before use. AIBN, used as a radical initiator, was recrystallized from ethanol solution. NVP was used as received and EGDMA was used as a cross-linker without further purification. Poly (ethy1ene glycol) (PEG) (Aldrich) with catalogue number-average molecular weights of 400, 600, 800, and 1000 (Aldrich) was dried by heating at 70 °C for 7 h under vacuum.

Preparation

The P(MMA-co-VP)/PEG semi-IPNs were prepared by radical polymerization and crosslinking of 37.5–59.5 wt% MMA and 26 wt% NVP in the presence of 0.5 wt% 2,2′-azobis(isobutyronitrile) (AIBN) as an initiator, 1–15 wt% ethylene glycol dimethacrylate (EGDMA) as a crosslinker, and 15–40 wt% linear PEG (MW:400, 600, 800, 1000). The reaction mixture was bubbled with nitrogen for 15 min. to remove the oxygen from the mixture, and then injected into the space between two glass plates separated by polyethylene spacers (3 mm thick) or into various alphabetic shapes' cylindrical glass tubes with a diameter 7 mm. Reaction was carried out at 55 °C for 24 h. The characteristics of the prepared polymer are summarized in Table 1. All specimens was quenched and then dried under vacuum at room temperature for 10 days to remove unreacted monomers. The weight loss during the drying process was negligible indicating that the monomer-to-polymer conversion was nearly 100%. According to the formulations of PEG content and compositions of P(MMA-co-VP)/PEG semi-IPNs, these polymers were represented as A (molecular weight of PEG) series, B (content of PEG) series and C (cross-linking density of network: the cross-linking density of the networks in this study uses only initial crosslinker concentration in the feed and was simply calculated as the molar ratio of cross-linking agent to the total monomer.) series, respectively.

Table 1 Characteristics of P(MMA-co-VP)/PEG semi-IPNs prepared

Notation	Cross-linking density (wt %)	PEG	
		MW	C (wt %)
A (Molecular weight of PEG) series			
A1	5.4	400	30
A2	5.4	600	30
A3	5.4	800	30
A4	5.4	1000	30
B (content of PEG) series			
B1	6.3	1000	15
B2	6.3	1000	30
B3	6.3	1000	35
B4	6.3	1000	40
C (Cross-linking density of network) series			
C1	1.0	1000	30
C2	3.7	1000	30
C3 (A4)	5.4	1000	30
C4	8.7	1000	30
C5	11.8	1000	30

Fourier transform infrared (FTIR) spectroscopy

FTIR spectra were obtained on a Nicolet 200XV FTIR spectrometer at a resolution of 2 cm^{-1}. A minimum of 16 scans were signal averaged. The dried samples were examined as pressed KBr disks.

Transmission electron microscope (TEM) observations

TEM measurements were carried out on a JEM-100CX Microscopy (Japan Electronic Company). Samples were prepared by dropping a suspension onto Formvar-coated copper grids.

Differential scanning calorimetry (DSC) measurements

The thermal analyses were carried out with a differential scanning calorimeter (DuPont 9900) over a temperature range from −70 °C to 150 °C at a heating rate of 10 °C /min, purged with nitrogen gas, and quenched with liquid nitrogen. The cell was calibrated using an indium standard; the weight of the sample was 5–10 mg.

Dynamic mechanical analysis (DMA)

The dynamic mechanical analyses were carried out with a DuPont 983 DMA at fixed oscillation amplitude of 0.1 mm using the single cantilever model and under nitrogen gas purging. A sheet of the sample (size: 60×12×2 mm) was heated from 10 °C to 200 °C using a heating rate of 2–3 °C /min.

Shape memory behavior

The method of evaluating the shape memory effect of the shape-memory alloy [25] was adopted to investigate that of our specimens. The shape memory effect was examined by a bending test as follows: a straight strip (size: 60×12×2 mm) of the specimen was folded above T_g (above T_g+ 20 °C) of the semi-IPNs, then cooled to keep the deformation under 25 °C. Then the deformed sample was heated again at a fixed heating rate of 5 °C /min from 20 °C to 180 °C and the change of the angle θ_f with temperature was recorded. The ratio of the recovery was defined as θ_f / 180. This process was designed a time series test.

Results and discussion

P(MMA-co-VP) networks were prepared and crosslinked by radical copolymerization of MMA with NVP in the presence of linear PEG. The obtained P(MMA-co-VP)/PEG is a kind of semi-interpenetrating polymer networks [28], i.e., crosslinked P(MMA-co-VP) network and linear PEG. Scheme 1 shows the synthesis route and the expected structure of P(MMA-co-VP)/PEG semi-IPNs.

FTIR spectroscopy analysis

FTIR was used to characterize the H-bond interaction between PVP and PEG. Carbonyl group on PVP and hydroxyl group on PEG are employed as hydrogen acceptor and donor, respectively. We pay special attention to absorption of OH group stretching vibrations, because these groups are most sensitive to hydrogen bonds. Figure 1 shows typical FTIR spectra of linear PEG, P(MMA-co-VP) networks and P(MMA-co-VP)/PEG semi-IPNs. For pure PEG600 (PEG, MW=600) and PEG1000, it can be seen in Fig. 1, the OH vibration presents a broad band centered around 3352 cm^{-1} and 3359 cm^{-1}; the band corresponding to absorption of a free OH group at 3640 cm^{-1} is absent in the PEG spectra[29]. This is because all hydroxyl groups of PEG form hydrogen bonds (intra- or intermolecular) and the hydrogen bond formation results form the interaction between the end hydroxyl and ether oxygen of the main chain, which makes the OH vibration shift to higher

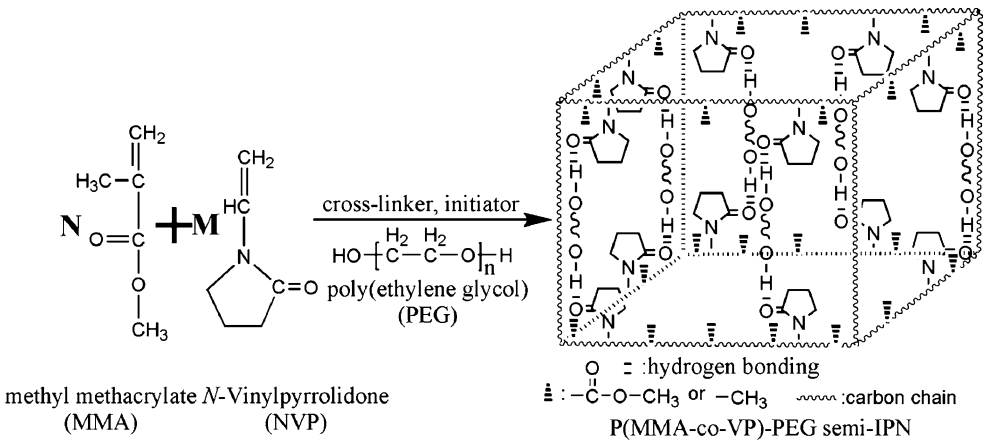

Scheme 1 Synthesis of P(MMA-co-VP)/PEG semi-IPNs

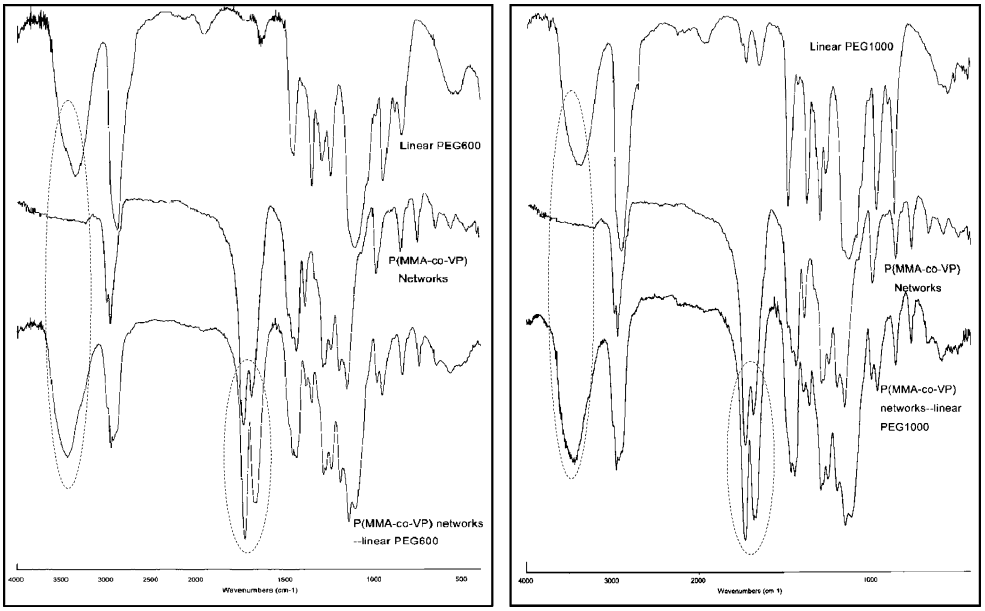

Fig. 1 FTIR spectra of PEG600, PEG1000, P(MMA-co-VP) networks, and P(MMA-co-VP)/PEG semi-IPNs

frequencies. For P(MMA-co-VP)/PEG semi-IPNs, compared to linear PEG, the OH vibration is shifted to a longer wavenumber of 3436 cm^{-1} for P(MMA-co-VP)/PEG600 semi-IPNs and of 3457 cm^{-1} for P(MMA-co-VP)/PEG1000 semi-IPNs, resulted from the H-bond between the PEG and PVP, forming a stronger hydrogen bond between PEG and PVP in the semi-IPNs than that in pure PEG.

A second region in relation to hydrogen bonds is that of the carbonyl group in PVP and PMMA, which is also shown in Fig. 1. For P(MMA-co-VP) networks, the vibration of PMMA and PVP carbonyl group appears around 1727 cm^{-1} and 1680 cm^{-1}, respectively. However, for P(MMA-co-VP)/PEG semi-IPNs, the frequency of the C=O stretching of the PVP is separated into two peaks centered at 1680.6 and 1666.7 cm^{-1} for P(MMA-co-VP)/PEG1000 semi-IPNs, and at 1679 and 1665.7 cm^{-1} for P(MMA-co-VP)/PEG600 semi-IPNs. The former was assigned to the vibrations of free carbonyl groups and the latter was assigned to hydrogen-bonded carbonyl groups. It is noteworthy that the frequency of C=O stretching of the PMMA does not change, indicating that the carbonyl group of PMMA may not take part in the formation of hydrogen bond. It can reasonable to conclude that the hydrogen bonds mainly exist in between the PEG hydroxyl group and the carbonyl group of PVP as shown in scheme 1.

Miscibility assessment using TEM and DSC

P(MMA-co-VP)/PEG semi-IPNs are transparent at room temperature. It is well known that PEG is a semicrystalline polymer with higher crystallinity and can show typical crystal diffraction pattern by TEM observations, corresponding to regular lattice structure, as shown in Fig. 2(a). P(MMA-co-VP)/PEG1000 semi-IPNs by radical copolymerization are amorphous, which shows an amorphous halo in Fig. 2(b), indicating that the characteristic of PEG crystal disappears and PEG is fully miscible with P(MMA-co-VP) networks. The existence of hydrogen bonds is in favor of dispersion of

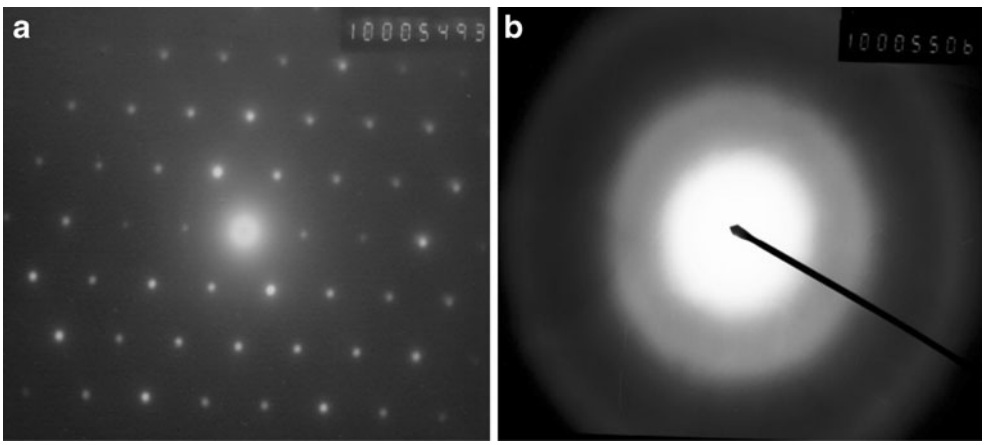

Fig. 2 TEM diffraction photographs. **a** PEG1000 homopolymer and **b** P(MMA-co-VP)/PEG semi-IPNs networks

PEG in P(MMA-co-VP) networks and destroys the structure of PEG crystal aggregates; so, P(MMA-co-VP)/PEG semi-IPNs exhibit homogeneous amorphous phase.

A simple and useful method to analyze the miscibility of PEG with P(MMA-co-VP)/PEG network is the determination of their glass transition temperatures (T_gs) using DSC. The thermograms of the series A semi-IPNs, the series B semi-IPNs and the series C semi-IPNs are shown Figs. 3, 4 and 5, respectively. Only one transition is observed for all P(MMA-co-VP)/PEG semi-IPNs; a single compositionally dependent glass transition is an indication of full miscibility at a dimensional scale between 20 and 40 nm[30], and implies full miscibility of the semi-IPNs.

It would be of interest to study the effects of chain length of PEG on the complexation with the P(MMA-co-VP) networks. Figure 3 suggests that the pure amorphous P(MMA-co-VP) network exhibits one T_g at ca. 125 °C and the P(MMA-co-VP)/PEG semi-IPNs display a single T_g. The addition of PEG to P(MMA-co-VP) network causes the depression of the T_g of PMMA network; the smaller the molecular weight of PEG, the more the decreased T_g.

We have also studied the influence of the PEG content on P(MMA-co-VP)/PEG semi-IPNs. As shown in Fig. 4, pure PEG1000 only shows the melting temperature without T_g. because PEG is easily crystallized and the content of the amorphous phase is very low [31]; thus, it is very difficult to measure the T_g of PEG in general. However, endothermic peaks due to the melting of PEG crystallites are not observed, and only one glass transition was exhibited corresponding to the P(MMA-co-VP)/PEG1000 semi-IPNs. These facts mean the crystalline phase of PEG1000 is destroyed in the complex and that there is only the amorphous phase in P(MMA-co-VP)/PEG semi-IPNs

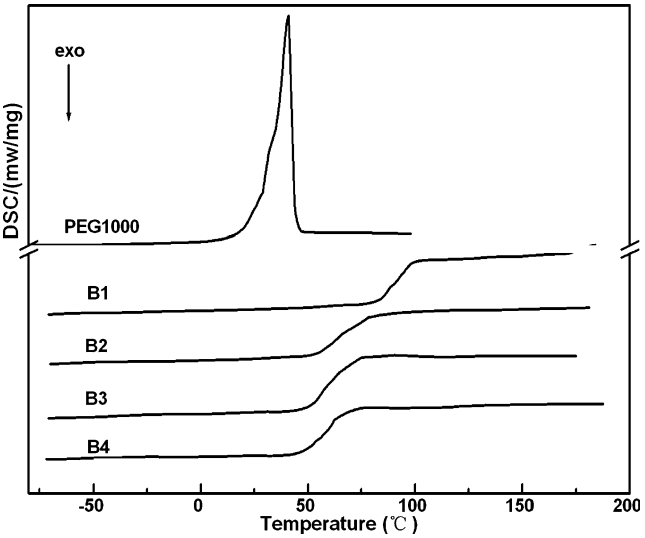

Fig. 4 DSC scans of series B semi-IPNs with various content of PEG

where the segments are molecularly mixed, in agreement with TEM analysis. The DMA result, discussed later, also suggests that the PEG–PVP complex phase is amorphous due to a single glass transition. In the case of T_g of the semi-IPNs, it decreases with increasing of PEG content, which may be interpreted in terms of the Fox equation.

The influence of cross-linking density on P(MMA-co-VP)/PEG semi-IPNs are presented in Fig. 5. It is worth noting that cross-linking density plays an important role for T_g of semi-IPNs. With increasing of cross-linking density of polymer networks, T_g of the semi-IPNs shifts to relatively high temperature. It is known that several factors can influence the T_g values of the crosslinked polymers: main chain rigidity, cross-linking density and the chemical

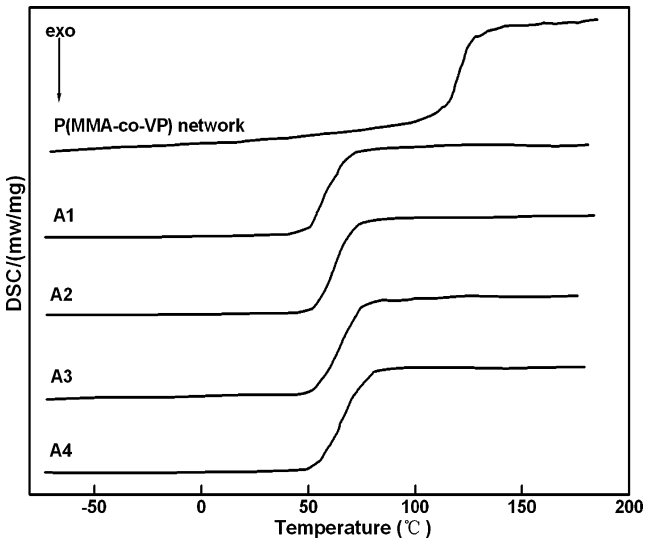

Fig. 3 DSC scans of P(MMA-co-VP) networks and series A semi-IPNs with various molecular weight of PEG

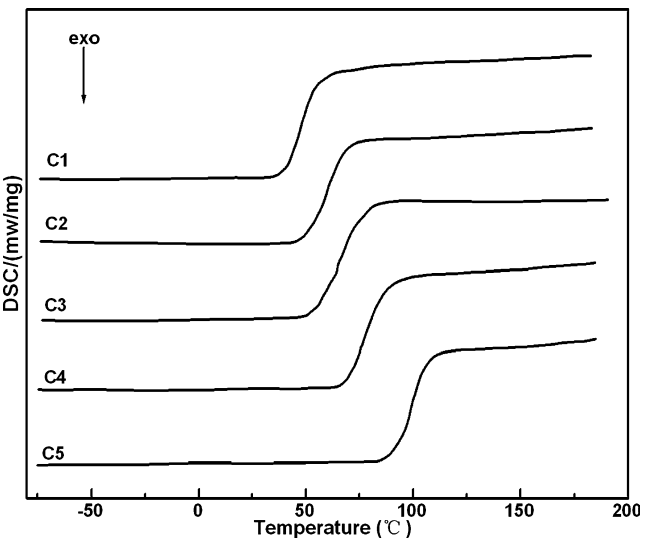

Fig. 5 DSC scans of series C semi-IPNs with various cross-linking densities

structure of the hardener introduced. Relatively high cross-linking densities restrict the motions of polymer chain and make T_g shift to a high temperature region.

Dynamic mechanical analysis (DMA)

It is well known that the dynamic mechanical analysis, which is sensitive to the molecular motion in polymer, could provide important information on thermal motions of chain segments. Parts a and b of Fig. 6 show the temperature dependence of the elastic storage E' and tanδ for P(MMA-co-VP) network and P(MMA-co-VP)/PEG semi-IPNs with various molecular weight of PEG, respectively. From Fig. 6a, it can be seen that, for all systems, the logarithm of the storage modulus, logE', varies very little in the first section of the curve, called the plateau zone. A sharp decrease for semi-IPNs is then observed and is attributed to the change in segment mobility related to the glass transition, while a relatively small difference is discovered in storage modulus for the P (MMA-co-VP) network. It can be noted that the average log E' values of the plateau increase gradually with the increasing of PEG molecular weight. This behavior may be explained by the changes of PEG storage modulus and it is believed that PEG storage modulus increase with increasing of PEG molecular weight.

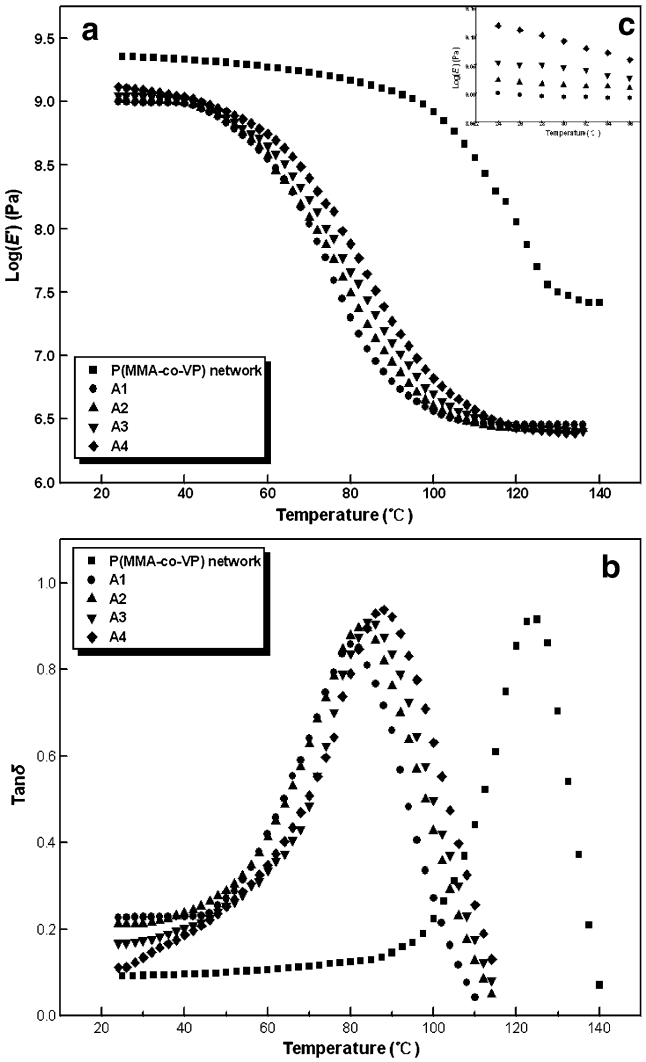

Fig. 6 Storage modulus (E') and loss tangent (Tanδ) for P(MMA-co-VP) network and series A semi-IPNs as a function of temperature

Polymers are viscoelastic materials which have some of the characteristics of both viscous liquids and elastic solids. When polymeric materials are deformed due to a periodic force, part of the energy is stored as potential energy and part energy is dissipated as heat by viscosity. The energy dissipated as heat resulting from molecular internal friction is reflected in the change in loss tangent (tanδ) of the dynamic mechanical behavior with temperature. In principle, the loss tangent maximum can be taken as the glass transition temperature [32]. From Fig. 6b, P(MMA-co-VP) network and P(MMA-co-VP)/PEG semi-IPNs display a single dynamic mechanical relaxation, indicating they are fully amorphous, in agreement with DSC analysis. Moreover, with increasing of molecular weight of PEG, maximum tanδ ($\tan_{max}\delta$) of semi-IPN shifts to high temperature, which is consistent with the DSC results; since the tanδ corresponds to the strain energy dissipated by viscous friction, a large tanδ implies that the material is more likely to be viscous than elastic.

The temperature dependence of the elastic storage E' and tanδ for P(MMA-co-VP)/PEG semi-IPNs with various content of PEG are shown in Fig. 7(a) and (b), respectively. From Fig. 7a, owing to the plasticizing effect of the introduced flexible PEG moieties, the plateau modulus of semi-IPNs decreases with increasing of PEG content. From Fig. 7b, with increasing of PEG content, $\tan_{max}\delta$ slightly shifts to low temperature, which coincides with previous findings as shown in Fig. 4.

The temperature dependence of the elastic storage E' and tanδ for P(MMA-co-VP)/PEG semi-IPNs with various cross-linking density is shown in Fig. 8. From Fig. 8a, the plateau modulus of semi-IPNs increases with increasing of cross-linking density. This is because higher cross-linking density increases the rigidity of semi-IPNs; a distinct decease in E' also occurred in the T_g region, similar to Figs. 6a and 7a. From Fig. 8b, $\tan_{max}\delta$ dramatically shifts to high temperature under the condition of high cross-linking density; this result is consistent with Fig. 5. Relatively high cross-linking densities restrict the motions of polymer chain and lead to a weak relaxation intensity.

Shape memory behavior

Based on results above, these P(MMA-co-VP)/PEG semi-IPNs could be a kind of shape memory polymer. We think

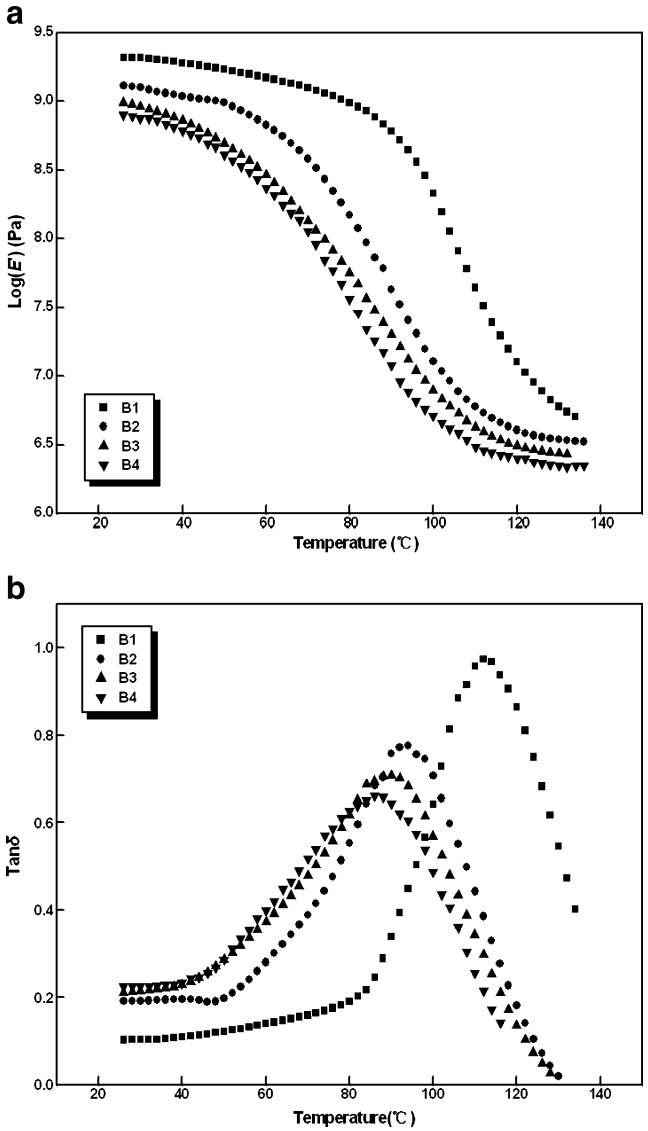

Fig. 7 Storage modulus (E') and loss tangent (Tanδ) for series B semi-IPNs as a function of temperature

that the shape memory behaviors of the semi-IPN might be associated with the high elasticity ratio of the glass state modulus to the rubbery modulus below and above T_g of P (MMA-co-VP)/PEG semi-IPNs.

We consider the differences in the dynamic mechanical properties between the P(MMA-co-VP) network and the P (MMA-co-VP)/PEG semi-IPNs could be interpreted in terms of cooperative inter-polymer hydrogen bonds which alter the dynamics and structures of the semi-IPNs. The existence of hydrogen bonds causes formation of physical network between PVP and PEG, which partially restricted the side chain movements of PVP and slightly increased the stiffness of P(MMA-co-VP)/PEG semi-IPNs at room temperature. When the semi-IPNs were heated to T_{trans} (above T_g+20 °C), they can transform from the glass state to rubber-elastic state, and, on the other hand, the hydrogen bonds between PVP and PEG, are broken. Moreover, the number of hydrogen bonds between the carbonyl groups of PVP and the terminal hydroxyl groups of PEG decreases with heating [33], which produces a decrease in the stiffness. All results above make the semi-IPNs flexible; the polymer is easily deformed under external force. When the semi-IPNs were cooled to room temperature, they return to glass state and the broken hydrogen bonds recombine [34], which favor the fixing of temporary shape. The maximum storage modulus ratio can be more than 400 for P (MMA-co-VP)/PEG semi-IPNs, while that of P(AA-co-MMA)-PEG complexes at best reach to 170 [24].

Shape memory polymers basically contain a fixing phase and a reversible phase. The fixing phase imparts a level of

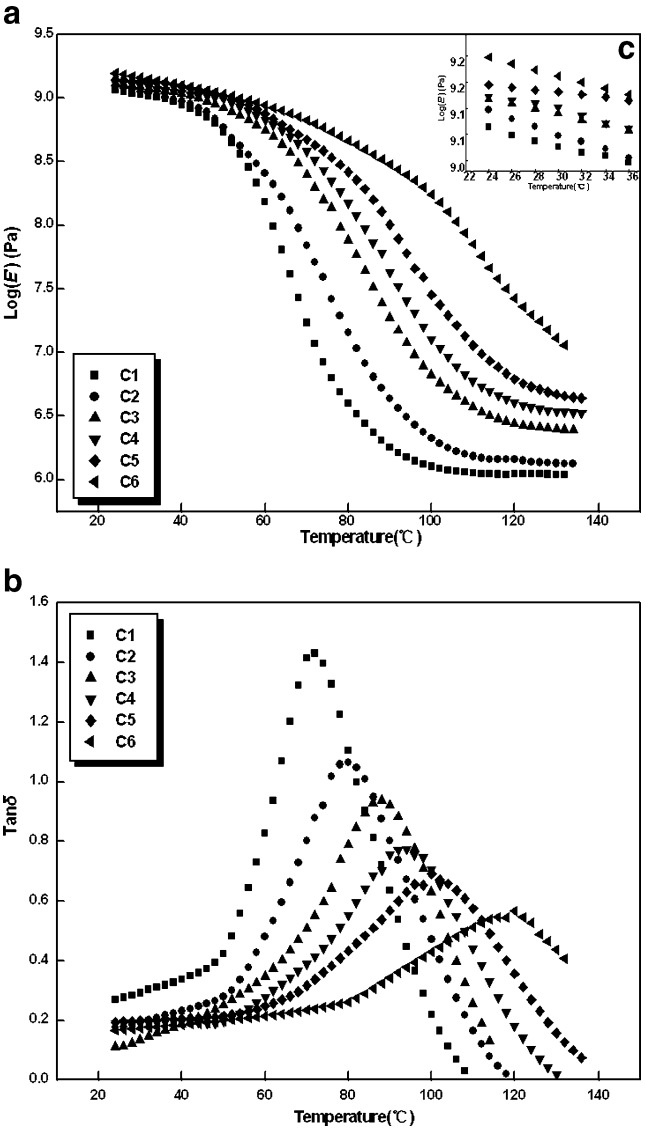

Fig. 8 Storage modulus (E') and loss tangent (Tanδ) for series C semi-IPNs as a function of temperature

rigidity, dimensional stability, and thermal resistance, while the reversible phase provides properties of elastomers—primarily recovery and energy absorption. Considering the P(MMA-co-VP)/PEG semi-IPNs, the fixing phase was the chemical crosslinked point, while the reversible phase was the PEG–PVP complex phase. By introducing PEG, the modulus of P(MMA-co-VP)/PEG semi-IPNs dramatically change below and above the transition temperature. Meanwhile, from Fig. 6(c), it can be seen that the glass modulus increased with increasing PEG molecular weight. This means that the modulus of the glass state of the semi-IPNs connect with the elastic energy of the amorphous PEG–PVP complex phase. A high glassy state modulus will provide the materials with high shape retention during cooling and unloading. Thus, the reversible phase transformation with a high glassy state modulus is responsible for the shape memory effect.

In Fig. 9, a picture sequence demonstrates impressively the performance of shape-memory P(MMA-co-VP)/PEG1000 semi-IPN. The permanent shape of the polymers is four alphabets of "c", "h", "e", and "m", i.e., "Chem", which has been deformed to four rods (temporary shape) under constrained conditions above 95 °C, followed by down to room temperature. Under the action of hot air with temperature of 95 °C, without the external force, the permanent shape is recovered within 45 s. This interesting phenomenon is reversible and cyclically reproduced by repeated temperature changes. Compared with P(MMA-co-VP)/PEG1000 semi-IPN, however, P(MMA-co-VP) networks do not show shape memory effect below 100 °C, as shown in Fig. 10.

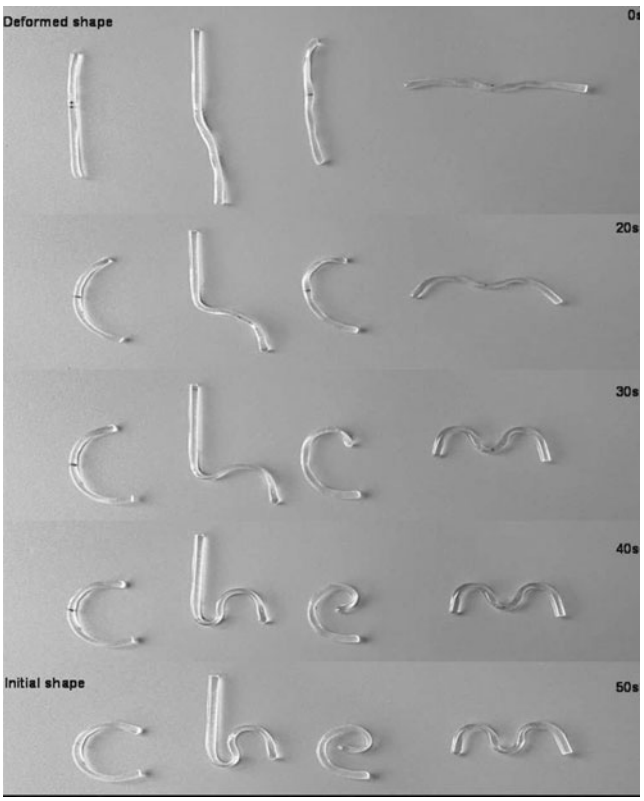

Fig. 9 Transition from the temporary shape (four rods) to the permanent shape ("Chem") for A4. The switching temperature of the polymer is 90 °C based on T_g. The recovery process takes 50 s after heating to 95 °C

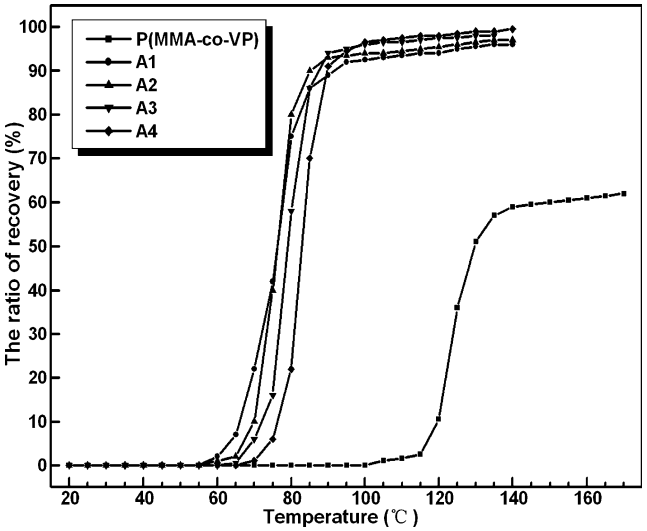

Fig. 10 Shape memory effect of P(MMA-co-VP) network and series A semi-IPNs

Shape memory behavior is detected in the temperature study, as shown in Fig. 10, and provides a direct comparison of the shape memory effect of P(MMA-co-VP)/PEG semi-IPNs and the P(MMA-co-VP) network. The data curves, based on the recovery ratio and temperature, are S-shaped. The deformation could be recovered relatively rapidly when the deformed sample was heated again to a

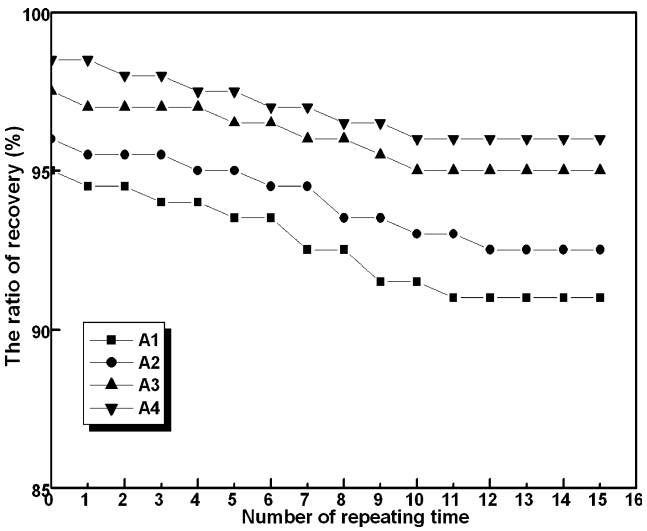

Fig. 11 Relationship between the ratio of recovery and the number of tests on series A semi-IPNs

high temperature. The ratio of recovery could reach nearly 100%; the network showed a slow recovery rate, but there was still residual deformation that was not recovered under the testing process. Semi-IPNs with higher PEG molecular weight showed a higher recovery rate than those with a lower PEG molecular weight. The PEG content has more or less influence on shape memory effect, mainly reflecting in T_g of semi-IPNs, as shown in Fig. 7. But the PEG content must be less than 50 wt%, otherwise P(MMA-co-VP)/PEG semi-IPNs is easily fragile and not suitable for being materials. It is worth noting that cross-linking density plays an important role for shape memory effect; on the one hand, higher cross-linking density increases glass modulus, as shown in Fig. 8(c), and T_g of semi-IPNs, which imparts the semi-IPNs a level of rigidity, dimensional stability, and thermal resistance; on the other hand, higher cross-linking density restricts chain mobility and makes a little change in rubbery modulus, as shown in Fig. 8(a), which gives an unfavourable contribution to high temperature deformation; when the cross-linking density is more than 15 wt%, P (MMA-co-VP)/PEG semi-IPNs hardly show shape memory effect in our system.

Figure 11 shows the results of the influence of the number of testing on the ratio of recovery for A4. The ratio of recovery is slightly reduced and then approximates to a steady value as the number of testing increased. Thus, A4 shows better shape memory behavior after a training process. The loss of recovery may be associated with the dissociation of the complex during the repeated temperature changes.

Conclusion

The thermal behaviors, crystalline morphology and dynamic mechanical properties of the P(MMA-co-VP)/PEG semi-IPNs was studied by DSC, TEM, and DMA, respectively. The semi-IPNs showed shape memory properties due to a large difference in storage modulus below and above the glass transition temperature. When PEG with a higher molecular weight was introduced into the network, (1) a higher glassy state modulus and (2) a higher recovering rate were obtained. The content of PEG and the cross-linking density of P(MMA-co-VP) network have the important influence on shape memory effect of this semi-IPNs. The shape memory effect can be easily modulated by varying the molecular weight of the PEG and the cross-linking density, which is very important in real applications.

Acknowledgment The authors acknowledge the National Natural Science Foundation of China (Grant No. 50373045) and the Opening Project of State Key Laboratory of Polymer Materials Engineering (Sichuan University) for financial support of this research.

References

1. Huang WM et al (2010) Mater Today 13:54–61
2. Lendlein A, Kelch S (2002) Angew Chem Int Ed 41:2034–2057
3. Liu C, Qin H, Mather PT (2007) J Mater Chem 17:1543–1558
4. Rousseau IA (2008) Polym Eng Sci 48:2075–2089
5. Ratna D, Karger-Kocsis J (2008) J Mater Sci 43:254–269
6. Gunes IS, Jana SC (2008) J Nanosci Nanotechnol 8:1616–1637
7. Liu Y, Lv H, Lan X, Leng J, Du S (2009) Compos Sci Technol 69:2064–2068
8. Mather PT, Luo XF, Rousseau IA (2009) Annu Rev Mater Res 39:445–471
9. Xie T (2010) Nature 464:267–270
10. Feninat FEL, Laroche G, Fiset M, Mantovani D (2002) Adv Eng Mater 4:91–104
11. Hu Z, Zhang X, Li Y (1995) Science 269:525–527
12. Osada Y, Matsuda A (1995) Nature 376:219–219
13. Lendlein A, Langer R (2002) Science 296:1673–1676
14. Lendlein A, Jiang HY, Junger O, Langer R (2005) Nature 434:879–882
15. Yang B, Huang WM, Li C, Li L (2006) Polymer 47:1348–1356
16. Sun L, Huang WM (2010) Soft Matter 6:4403–4406
17. Lv HB, Leng JS, Liu YJ, Du SY (2008) Adv Eng Mater 10:592–595
18. Samra K, Galaev IY, Mattiasson B (2000) Angew Chem Int Ed 39:2364–2367
19. Ratna D, Karger-Kocsis J (2008) J Mater Sci 43:254–269
20. Tobushi H, Hayashi S, Hoshio K, Miwa N (2006) Smart Mater Struct 15:1033–1038
21. Kelch S, Steuer S, Schmidt AM, Lendlein A (2007) Biomacromolecules 8:1018–1027
22. Sokolowski W et al (2007) Biomed Mater 2:S23–27
23. Guan Y, Cao YP, Peng YX et al (2001) Chen Chem Commun 17:1694–1695
24. Cao YP, Guan Y, Du J, Luo J, Peng YX et al (2002) J Mater Chem 12:2957–2960
25. Liu GQ, Ding XB, Cao YP, Zheng ZH, Peng YX (2004) Macromolecules 37:2228–2232
26. Tsuchida E, Abe K (1982) Adv Polym Sci 45:1–119
27. Feldstein MM, Kuptsov SA, Shandryuk GA, Platé NA (2001) Polymer 42:981–990
28. Cesteros LC, Quintana JR, Fernandez JA, Katime I (1989) J Polym Sci Polym Phys Ed 27:2567–2576
29. Sperling LH, Mishra V (1996) Polym Advan Technol 7:197–208
30. Philippova E, Kuchanov SI, Topchieva IN, Kabanov VA (1985) Macromolecules 18:1628–1633
31. Kuo SW, Chang FC (2001) Macromolecules 34:4089–4097
32. Kafoglou NK, Sotiropoulou DD, Margaritis AG (1988) Eur Polym J 4:389–394
33. Eisenberg A (1993) In physical properties of polymers, 2nd edn. American Chemical Society, Washington, DC, p 70
34. Zhang Y, Guan Y, Yang S, Xu J, Han CC (2003) Adv Mater 15:832–835